Variable-Density Oblique Spherical Navigator Echoes to Improve Performance in Measuring 3D Motion

A. F. Costa[1,2], D. Petrie[1,2], M. Drangova[1,2]

[1]Robarts Research Institute, London, Ontario, Canada, [2]Department of Medical Biophysics, The University of Western Ontario, London, Ontario, Canada

Introduction: Correcting for subject motion remains a challenging problem in Magnetic Resonance Imaging. One-dimensional navigator echoes have been used successfully in a number of applications, but can only measure translations in one direction. Spherical navigator (SNAV) echoes have the potential to accurately measure and correct for rigid-body motion in 3D, however, several design considerations in the acquisition of helical-spiral SNAVs can greatly affect the overall performance of this technique. For example, the slew rate limitation prevents acquisition of the poles of the spherical shell for typical combinations of sampling density and k-space radius (1). In addition, higher accuracy is attained in SNAV registration when the rotations are predominantly along the threads of the helical-spiral trajectory, rather than "cross-thread" (2). In this study we tested modifications to the SNAV trajectories that overcome the slew rate limitation and acquire points on the entire spherical shell. The modified trajectories were found to improve upon the SNAV technique's accuracy in detecting 3-dimensional compound rotations by up to one degree rms.

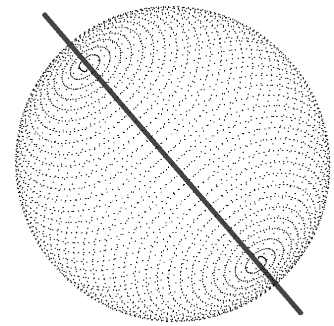

Fig. 1: An oblique SNAV. The equatorial plane is normal to the line $k_x=k_y=k_z$ to distribute the demands on the gradients and not exceed the max. slew rate.

Theory: The helical-spiral SNAV trajectories described in (2) acquire data over 85% of the spherical shell, stopping short of collecting data on the "poles" of the k-space sphere to avoid exceeding the maximum slew rate. Our first modification implemented a variable-density sampling method along the 1-dimensional helical spiral. As the trajectory spiraled up to the poles of the sphere, the sampling density was increased, keeping the rate of change of the gradient magnitude beneath the maximum slew rate. Our second modification was to rotate the variable-density SNAV trajectories such that the poles of the spherical shell were intersected by the line $k_x=k_y=k_z$ (Fig. 1). These "oblique" SNAVs evenly distribute the demands on the G_x, G_y, and G_z gradients, do not exceed the maximum slew rate, and allow for the acquisition of evenly spaced points on the entire spherical shell. Another advantage to acquiring the SNAVs in an oblique plane is the increased magnitude of the G_z gradient, which can otherwise be on the same order as shimming gradients (Fig. 2).

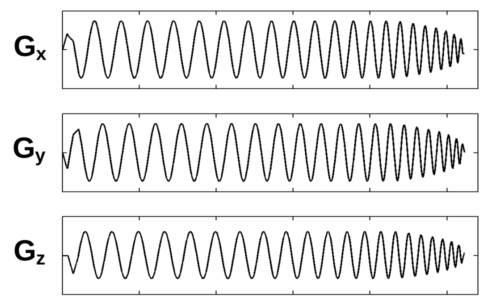

Fig. 2: The gradient waveforms used to generate the SNAV trajectory in Fig. 1 have similar amplitudes.

Methods: These developments were applied to three acquisition strategies that tested:

1) axial SNAVs that collected data on 85% of the sphere;
2) variable-sampling density (VSD) SNAVs that acquired data on the entire shell;
3) oblique VSD SNAVs that had their poles intersected by the line $k_x=k_y=k_z$.

The acquisition strategies were tested for their ability in detecting four compound rotations of varying magnitude. Although typical navigator studies collect echoes before and after applying experimental rotations to a phantom, in this experiment we rotated the *spherical navigator echo trajectories themselves*, rather than a phantom, to test their performance. This allowed us to apply highly accurate and precise rotations, with experimental errors being attributed to shimming, gradient delays, and other hardware imperfections. A human skull phantom filled with agar was kept stationary throughout. The four compound rotations consisted of components about all three axes, and ranged from 0-10°. To assess the precision of the three strategies, each trajectory was acquired 32 times. All SNAVs had the same radius (k_ρ = 0.4 cm^{-1}) and approximately equal sampling density (~ 2400 pts).

Results & Discussion: The accuracy of the SNAV acquisition strategies is presented in Fig. 3. Overall, the revised acquisition strategies improve upon the accuracy of the SNAV technique in detecting compound rotations. For the oblique SNAVs, which equally distribute the demands on the scanner gradients, the accuracy was improved by over one degree in rotation 2. All strategies exhibited precision of approximately 0.1°. It is evident, however, that the SNAV technique typically displays decreased accuracy for compound rotations, possibly because the minimization algorithm converged to local minima. Similar experiments revealed that all of the above strategies could accurately detect purely "along-thread" rotations to 0.10 +/- 0.03°, which indicates the dependency of the SNAV technique on the complexity of the rotations studied. Designs that reduce this dependence, such as perhaps pre-rotating the base-line dataset, may further improve the performance of this technique in detecting 3D motion.

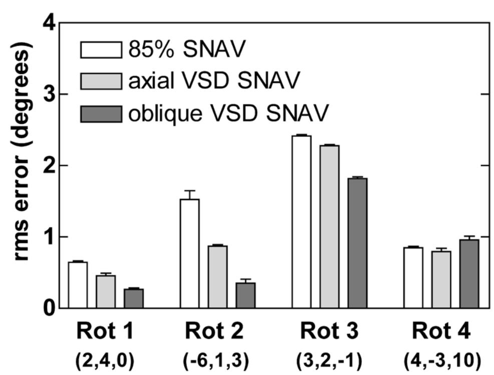

Fig. 3: The accuracy of the three strategies. The root mean squared error is calculated by comparing the three Euler angles (θ_x, θ_y, θ_z) found by the algorithm to the rotations shown.

Acknowledgements: The authors thank Dr. Atsushi Takahashi for valuable insights and the Canadian Institutes of Health Research and the Natural Sciences and Engineering Research Council of Canada for financial support.

References:

1. Welch EB, *et al.* Fast Helical-Spiral Spherical Navigator Echoes for 3-D Motion Detection and Inter-Scan Alignment. In: Proceedings of the 11th annual meeting of ISMRM, Toronto, Canada, 2003, p.1056.
2. Welch EB, *et al.* Spherical Navigator Echoes for Full 3D Rigid Body Motion Measurement in MRI. Magn Reson Med 2002; 1: 32-41.